Chapter 2
Clay Minerals as Natural Nanosheets

Robert A. Schoonheydt and Yasushi Umemura

2.1 Introduction

Particles with nanometer dimensions (nanoparticles) are all around us. The finest particles of sand are blown by the wind over thousands of kilometers. The finest particles of soils are either eroded by the wind in extremely dry conditions or by water under wet conditions and deposited hundreds of kilometers or more from the origin. The air contains nanoparticles of carbon, ice, and oxides and is often contaminated with organic and inorganic compounds. As natural layered silicates, clay minerals, are available everywhere and cheap, they have been mixed with organic polymers as bulking fillers in the industry. On the other hand, intercalated compounds of layered clay mineral, such as smectite, with organic molecules have been studied in the academia. The intercalated compounds are expecting to have hybridized characters and properties, which are something alike to those of the parent compounds; clay minerals and guest organic molecules, but something different from those of them.

Among these nanoparticles in nature, clay minerals take a unique position, not only because of their nanometer size but also because of their shape (clay minerals are layered materials or two-dimensional (2D) materials), ion exchange, and adsorption properties. These properties are the basis for intense research in the transformation of clay minerals into nanomaterials for a variety of technological application and in the incorporation of clay minerals in nanodevices. As clay minerals are natural materials that can be mined, they are cheap. But this comes at a

R.A. Schoonheydt (✉)
Department of Microbial and Molecular Systems, Kuleuven,
Kasteelpark Arenberg 23, 3001 Leuven, Belgium
e-mail: robert.schoonheydt@telenet.be

Y. Umemura
Department of Applied Chemistry, National Defense Academy,
Hashirimizu 1-10-20, Yokosuka, Kanagawa 239-8686, Japan

© Springer Japan KK 2017

T. Nakato et al. (eds.), *Inorganic Nanosheets and Nanosheet-Based Materials*,
Nanostructure Science and Technology, DOI 10.1007/978-4-431-56496-6_2

price in which they invariably contain impurities that may be harmful for the technological application envisaged. Synthetic clay minerals of high purity are also available and deserve to be investigated for possible application in the nanotechnological area.

2.2 Clay Minerals

2.2.1 General

Clay minerals form a group of layered silicates or phyllosilicates. The elementary building unit is the layer. It consists of sheets of corner-shared SiO_4^{4-} tetrahedral and edge-shared Al or Mg, [Al, Mg O_{6-n} $(OH)_n$] octahedra. These sheets are joined by common O atoms. 1:1 clay minerals have a layer, which consists of one sheet of Si tetrahedral and one sheet of Al or Mg octahedra. 2:1 clay minerals consist of one sheet of Al or Mg octahedral sandwiched between two sheets of Si tetrahedral.

Isomorphous substitution is the partial replacement of Si^{4+} in the tetrahedral sheets by cations of about the same size and one unit of charge less. Examples are Al^{3+} and Fe^{3+}. Isomorphous substitution also occurs in the octahedral sheets. Thus, Al^{3+} can be substituted by Mg^{2+}, Fe^{3+} or Fe^{2+}, and Mg^{2+} by Li^{+}. As a result not all the negative charges of the O atoms are neutralized by the cations. The clay mineral layer carries a negative charge, which is compensated by cations at the surface of the layers, the exchangeable cations.

Clay minerals occur in nature, but may also be synthesized. Table 2.1 summarizes the most common 1:1 and 2:1 clay minerals. They are subdivided into dioctahedral and trioctahedral clay minerals, respectively, with an Al octahedral sheet and a Mg octahedral sheet in the layer. The table gives the common name of the clay mineral, the chemical formula of the pseudo-unit cell, and the degree of isomorphous substitution x.

When $x = 0$ there is no isomorphous substitution and there are no exchangeable cations. When $x = 0.2–0.6$, exchangeable cations compensate the negative layer charge. They are hydrated and located in the interlayer space. The distance between

Table 2.1 Clay minerals: structural formulae, degree of isomorphous substitution and names

Degree if isomorphous substitution, x	Structural formula	Name
$x = \approx 0$	$[Si_2Al_2O_5(OH)_4]$	Kaolinite
$x = \approx 0$	$[Si_2Mg_3O_5(OH)_4$	Serpentine
$x = \approx 0$	$[Si_4Al_2O_{10}(OH)_2]$	Pyrophillite
$x = \approx 0$	$[Si_4Mg_3O_{10}(OH)_2]$	Talc
$x = 0.2–0.6$	$[Si_4Al_{2-x}Mg_xO_{10}(OH)_2]xM^+$	Montmorillonite
$x = 0.2–0.6$	$[Si_{4-x}Al_xAl_2O_{10}(OH)_2]xM^+$	Beiddelite
$x = 0.2–0.6$	$[Si_4Mg_{3-x}Li_xO_{10}(OH)_2]xM^+$	Hectorite
$x = 0.2–0.6$	$[Si_{4-x}AlxMg_3O_{10}(OH)_2]xM^+$	Saponite

successive layers is then determined by the thickness of the layer, the exchangeable cation, and the amount of water in the interlayer space. The layer thickness is constant. It is 0.76 nm for 1:1 clay minerals and 0.96 nm for 2:1 clay minerals. The interlayer distance is however variable and depends on the amount of water in the interlayer space. In dilute aqueous dispersions, the amount of water taken up by the clay minerals is so large that the clay minerals layers are completely separated into individual layers, diffusing randomly and independently in water. One says that the clay mineral is completely dispersed. The increase of the interlayer distance with water content is called swelling and the clay minerals are called swelling clay minerals or smectites. This is the case for 2:1 clay minerals with x = 0.2–0.6. If the degree of isomorphous substitution x is in the range 0.6–0.9, the 2:1 clay minerals can take up one or two water layers in the interlayer space, but cannot reach the fully dispersed state. These clay minerals are called vermiculites. 2:1 Clay minerals with x = 0.9–1 are called micas. They do not take up water in the interlayer space. In this chapter, we concentrate our discussion on smectites.

2.2.2 Smectites

Figure 2.1 shows the structure of one layer of a dioctahedral smectite. The 2:1 clay mineral layer consists of four layers of O atoms with Si atoms between the first and second layer and between the third and fourth layer and Al atoms (Mg in the case of trioctahedral 2:1 clay minerals) between the second and third layer. The negative charge of the layer, due to isomorphous substitution, is compensated by exchangeable cations at the surface of the layer. Oxygen atoms at the edges may also carry a negative charge that is compensated by H atoms, thus giving Si–OH, Al–OH, or Mg–OH groups. These hydroxyl groups undergo acid–base equilibria in aqueous dispersion:

$$\mathrm{M{-}OH} + \mathrm{H_3O^+} \rightleftarrows \mathrm{M{-}OH_2^+} + \mathrm{H_2O}$$

$$\mathrm{M{-}OH} + \mathrm{H_2O} \rightleftarrows \mathrm{M{-}O^-} + \mathrm{H_3O^+} \quad (\mathrm{M{=}Si,\ Al,\ or\ Mg})$$

In acid medium they take up a proton, while in basic medium they release a proton in solution. Thus, edges may be positively charged or negatively charged depending on the pH conditions.

Smectites are extracted from clays by fractionation or a combination of mild acid treatment and fractionation. The size fraction less than 2 μm is considered as the pure smectite fraction. Figure 2.1 shows AFM pictures of Langmuir–Blodgett (LB) films of saponite, hectorite, and montmorillonite. One observes layers of different sizes and shapes. Hectorite consists of lath-like layers; montmorillonite has plate-like layers, while saponite has both types. The white spots might be clay mineral particles or impurities attached to the clay mineral layers.

Synthetic smectites are also available. One avoids impurities such as quartz or calcite. The particle size of synthetic smectites can be tuned by the synthesis conditions. The best known is probably Laponite, a synthetic hectorite. It consists of very small particles, 30–50 nm. Dispersions of Laponite easily form gels. F-hectorite is obtained by melt synthesis followed by annealing to improve charge homogeneity and phase purity [1, 2]. Table 2.2 gives the synthetic smectites most often encountered in the scientific literature.

Ion exchange is one of the most important properties of smectites. The reaction is usually performed in water and the smectite is swollen to a partially dispersed state. It is then possible to introduce almost any type of cation, organic or inorganic, irrespective of its size. In the case of alkylammonium cations, the surface of the smectite layers is fully covered with alkyl chains. The clay mineral layers adopt a hydrophobic character. The alkyl chains take a specific orientation depending on

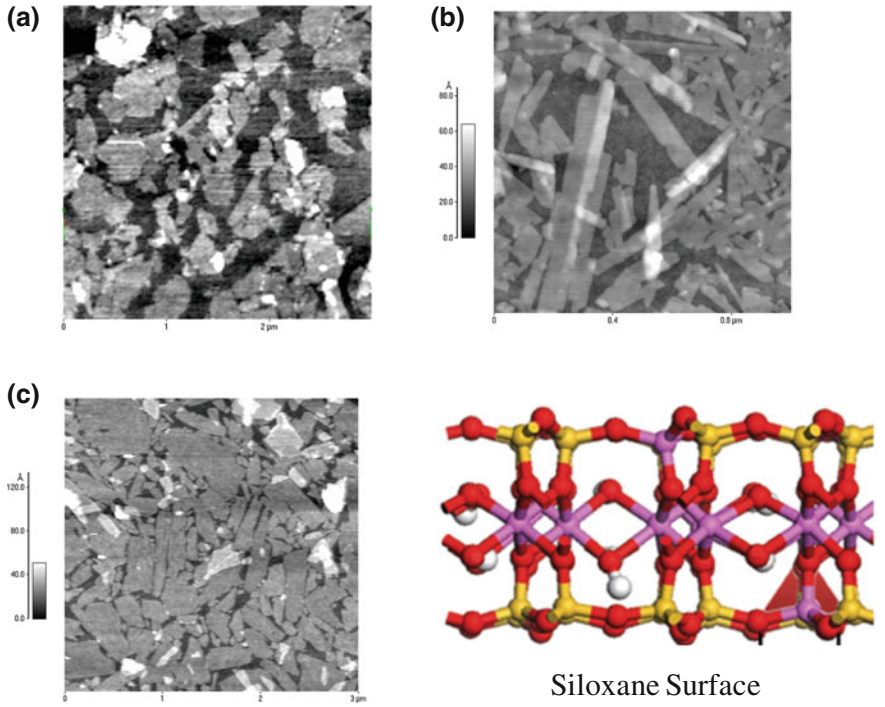

Fig. 2.1 Structure of one layer of a smectite: AFM pictures of single layers and particles (*white areas*) of **a** saponite, **b** hectorite, and **c** montmorillonite

Table 2.2 Examples of synthetic smectites

Name	Natural analog	Structural formula
Laponite	Hectorite	$[(Si_4)(Mg_{2.5}Li_{0.5})O_{10}(OH)_2]Na_{0.5}$
Fluor-hectorite	Hectorite	$[(Si_4)(Mg_{2.5}Li_{0.5})O_{10}(OH)_2]Na_{0.5}$
Smecton	Saponite	$[(Si_{3.6}Al_{0.4})(Mg_{2\cdot 99}Al_{0.01})O_{10}(OH)_2]Na0_{.25}Mg_{0\cdot 07}$

their length and on the charge density x of the layers. A schematic drawing is given in Fig. 2.2.

The lesson to be learnt is that molecules can be organized in the interlayer space of smectites. If these molecules carry a functionality such as a dipole moment, the resulting dipole moment of a single smectite layer may be zero or different from zero depending on the specific organization of the dipole moments in the interlayer

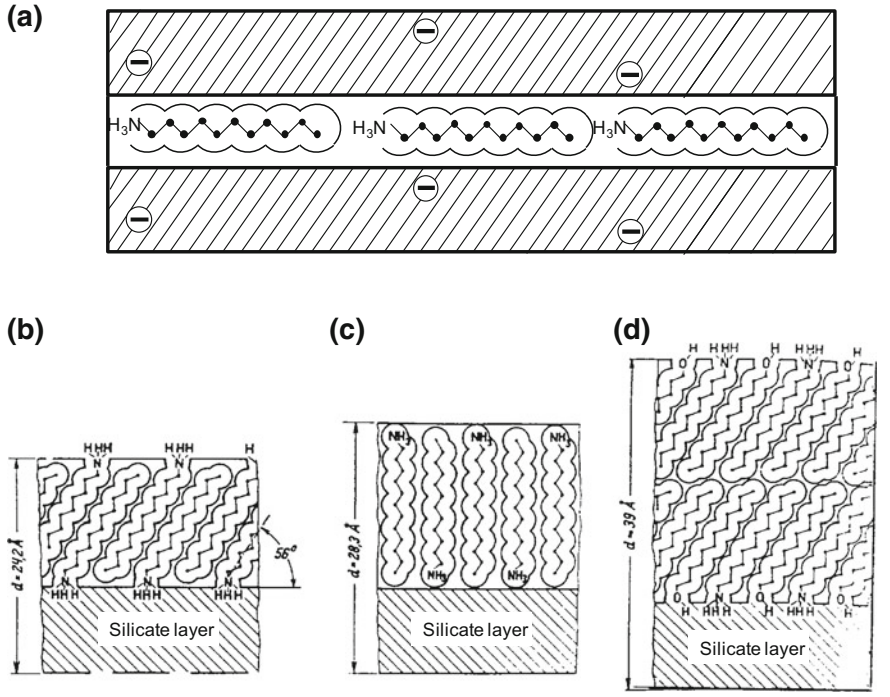

Fig. 2.2 Orientation of alkylammonium cations in the interlayer space of a smectite

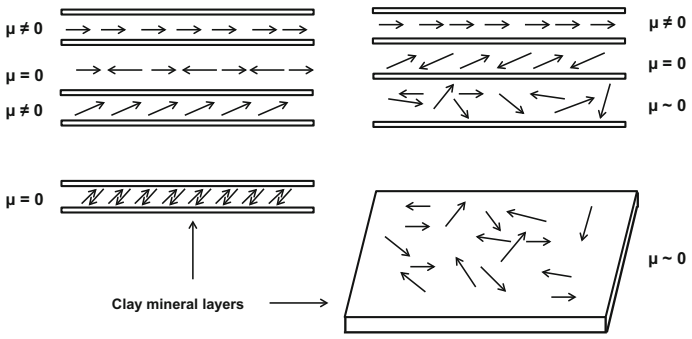

Fig. 2.3 Examples of arrangement of dipolar molecules in the interlayer space: ordered arrangements at the *left hand side*; disordered arrangements at the *right side*

space. If single layers each carrying a net dipole moment are organized in a film, the film may or may not have a dipole moment depending on the organization of the layers in the film (Fig. 2.3). Thus in order to prepare functional films, organization at two levels is required: (1) organization of the functional molecules at the surface of the clay mineral layers; (2) organization of the clay mineral layers themselves. There are four groups of methods to do so: casting, spin coating, layer-by-layer assembly, and Langmuir–Blodgett.

2.3 Film Formation Techniques

2.3.1 Casting

Casting is the deposition of an aqueous dispersion of clay minerals, followed by removal of excess water. It can be achieved in different ways, two of them are illustrated in Fig. 2.4. A few drops of the dispersion can be deposited on a hydrophobic surface. Upon slow drying in air at room temperature, a continuous film is formed with thickness in the mm range. While the dispersion is slowly drying, the clay mineral layers settle under the influence of gravitational forces with their surfaces parallel to the surface of the substrate. The result is a film with organized clay mineral layers. It can be used in X-ray diffraction (XRD) studies, Fourier Transform Infrared Spectroscopy (FTIR), electron paramagnetic resonance (EPR), and others. The orientation of structural OH groups of adsorbed molecules

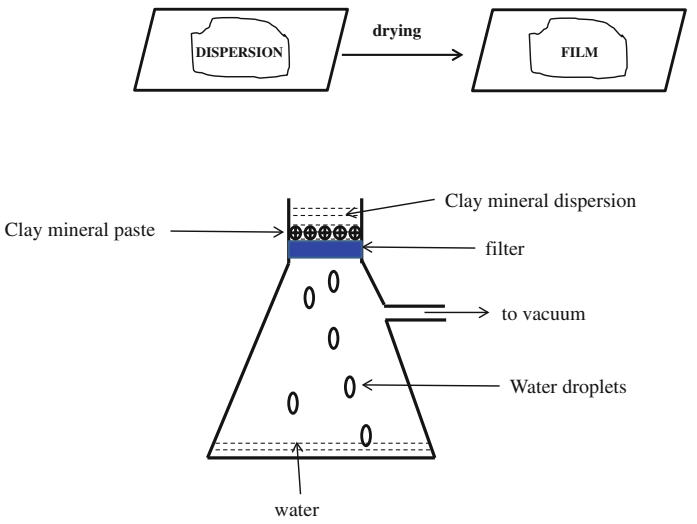

Fig. 2.4 Examples of film casting. *Upper part* Drying of a spread clay mineral dispersion. *Lower part* Suction of water out of a clay mineral dispersion

and of transition metal ion complexes at the interlayer surfaces can be studied with these films. The aqueous smectite dispersion can also be put on a filter paper with small pores and the excess water can be sucked away. What remains on the filter is a cake with oriented clay mineral layers and particles, which can be dried in air at room temperature.

2.3.2 *Spin Coating*

A few drops of the aqueous dispersion of a smectite are put on a disk, which is subsequently rotated. The dispersion is equally spread over the surface of the disk due to the centrifugal forces of the rotation. The solvent evaporates simultaneously, thus forming a film. The thickness of the film is dependent on the mass% of smectite in the aqueous dispersion and on the rotation speed. This is illustrated in Fig. 2.5 for Laponite. For 1 mass% dispersion, the film thickness decreases from ≈20 to ≈10 nm upon increasing the rotation speed from 400 to 1000 rpm (rounds per minute). For 2 mass% dispersions, the film thickness decreases from 60 to ≈30 nm with the rotation speed increasing from 400 to 1000 rpm.

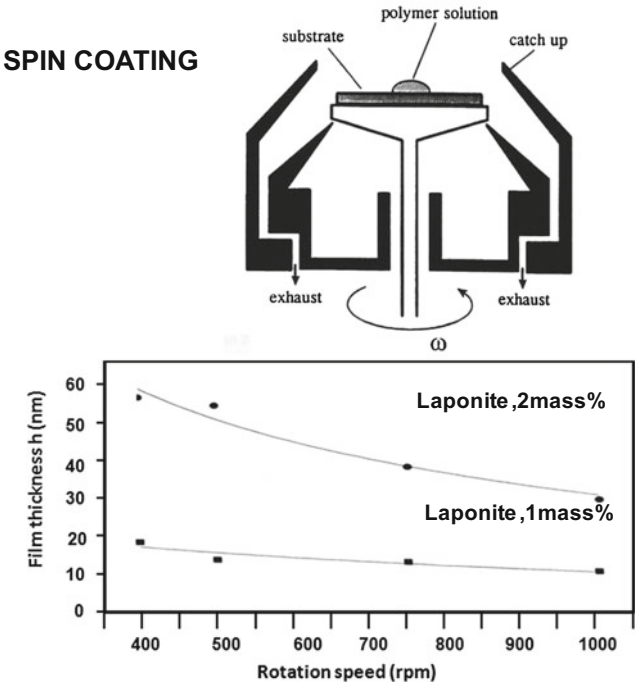

Fig. 2.5 *Upper part* Scheme of a spin coating apparatus. *Lower part* Film thickness as a function of the rotation speed for 2 mass% and 1 mass% Laponite dispersions

With spin coating one can also construct films, consisting of alternating layers of two different materials. Thus, alternating layers of Laponite and of a material with high refractive index such as TiO_2 result in a material with an optical band gap. As the Laponite layer is porous and the TiO_2 layer is not, the band gap properties can be influenced by adsorption of molecules in the Laponite layer. Such photonic band gap materials can then be used as sensors [3, 4].

2.3.3 *Layer-by-Layer (LbL) Assembling*

The principle of the technique is shown in Fig. 2.6. A substrate with a negatively charged surface is alternatively immersed in a solution of cationic polymers and in a dilute aqueous clay mineral dispersion. After each deposition the deposited layers are rinsed with water to remove excess material. This results in deposition of alternating layers of polymers and smectite layers and particles. One layer of polymer and one layer of clay mineral particles form a bilayer. These bilayers are held together mainly by electrostatic forces, as the polymer is positively charged and the clay mineral layers are negatively charged. The anions accompanying the cationic polymer and the exchangeable cations of the clay mineral layers and particles are free and are removed in the washing steps. The result is an ion exchange of a cationic polymer on the clay mineral surfaces.

The number of bilayers deposited can be increased, in principle infinitely, but not in practice. Indeed, the thickness of the films increases linearly with the number of bilayers, but this is not the case for the roughness of the films. Film roughness is defined as

$$\text{Roughness} = \left[\frac{\Sigma(h_i - h_a)^2}{n-1}\right]^{1/2},$$

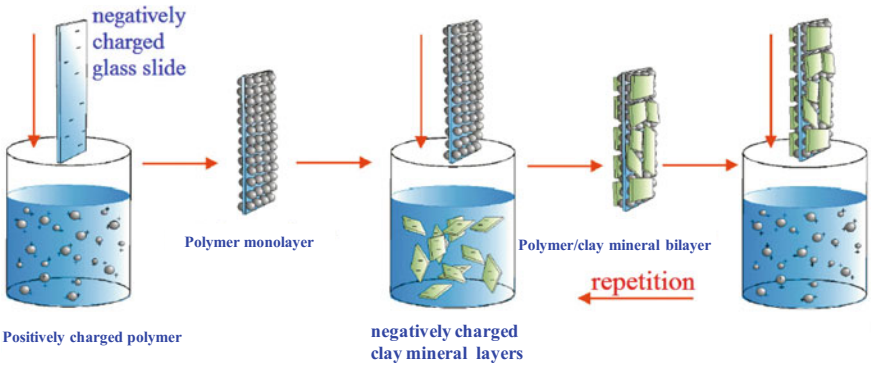

Fig. 2.6 The principle of layer-by-layer assembling

where h_i is the thickness of the film at point i, h_a is the average film thickness, and n is the number of datapoints.

It is observed that the roughness of the films increases with the concentration of poly(dialkyldimethylammonium) (PDDA) in solution and with the number of bilayers deposited. The roughness is also dependent on the particle size of the clay minerals [5]. For Laponite with particle sizes around 30 nm, the roughness is 4 nm or less after deposition of 20 bilayers, while it is 3–4 times higher for hectorite. After deposition of 20 bilayers the hectorite films are about 60 nm thick. A roughness of 12 nm is 20% of the film thickness. Thus hybrid LbL films of smectites and cationic polymers are not atomically smooth. The reasons for this are: (1) presence of clay mineral layers and particles; (2) sub-monolayer coverage for each deposition of clay mineral layers and particles; (3) overlap of clay mineral layers and particles in the film; (4) aggregation of clay mineral layers and particles in the PDDA matrix.

2.3.4 *Langmuir–Blodgett (LB) and Langmuir–Schaefer (LS) Technique*

The thickness of a 2:1 clay mineral layer is 0.96 nm and if a film is composed of these single clay mineral layers, it would be thin and smooth at the nanometer level. The LB and LS techniques have been applied to prepare such films. The procedures are illustrated in Fig. 2.7.

Clay mineral particles that are intercalated with amphiphilic cations such as alkylammonium cations are hydrophobic. They swell in organic solvents and form dilute dispersions of individual layers, analogously to the swelling of hydrophilic smectites in water. These dilute dispersions of hydrophobic smectite layers can be spread at the air–water interface. After evaporation of the solvent, the individual clay mineral layers are left at the interface. The floating individual layers can be gathered by barriers to form a film, as shown in Fig. 2.7a. The ultrathin film of packed clay mineral layers is then transferred to a substrate by vertical lifting (LB technique) or horizontal lifting (LS technique) [6, 7].

A second way of film preparation is spreading a solution of amphiphilic cations in a volatile organic solvent on a dilute aqueous clay mineral dispersion (Fig. 2.7b). The volatile solvent evaporates and the negatively charged smectite layers interact with the positively charged amphiphilic cations at the air–water interface. A floating hybrid monolayer is formed, consisting of clay mineral layers and amphiphilic cations. This floating monolayer is compressed and transferred on a substrate by vertical or horizontal lifting. Multilayers can be prepared by repeating the deposition procedure [8, 9]. This type of LB or LS film preparation is very versatile and therefore a promising technique for preparation of functional ultrathin films [10–12]. First, the layered structure of these hybrid multilayers is far more stable than those of conventional LB and LS films. Second, the density of amphiphilic cations on the clay mineral layers in the film is controlled by changing the clay

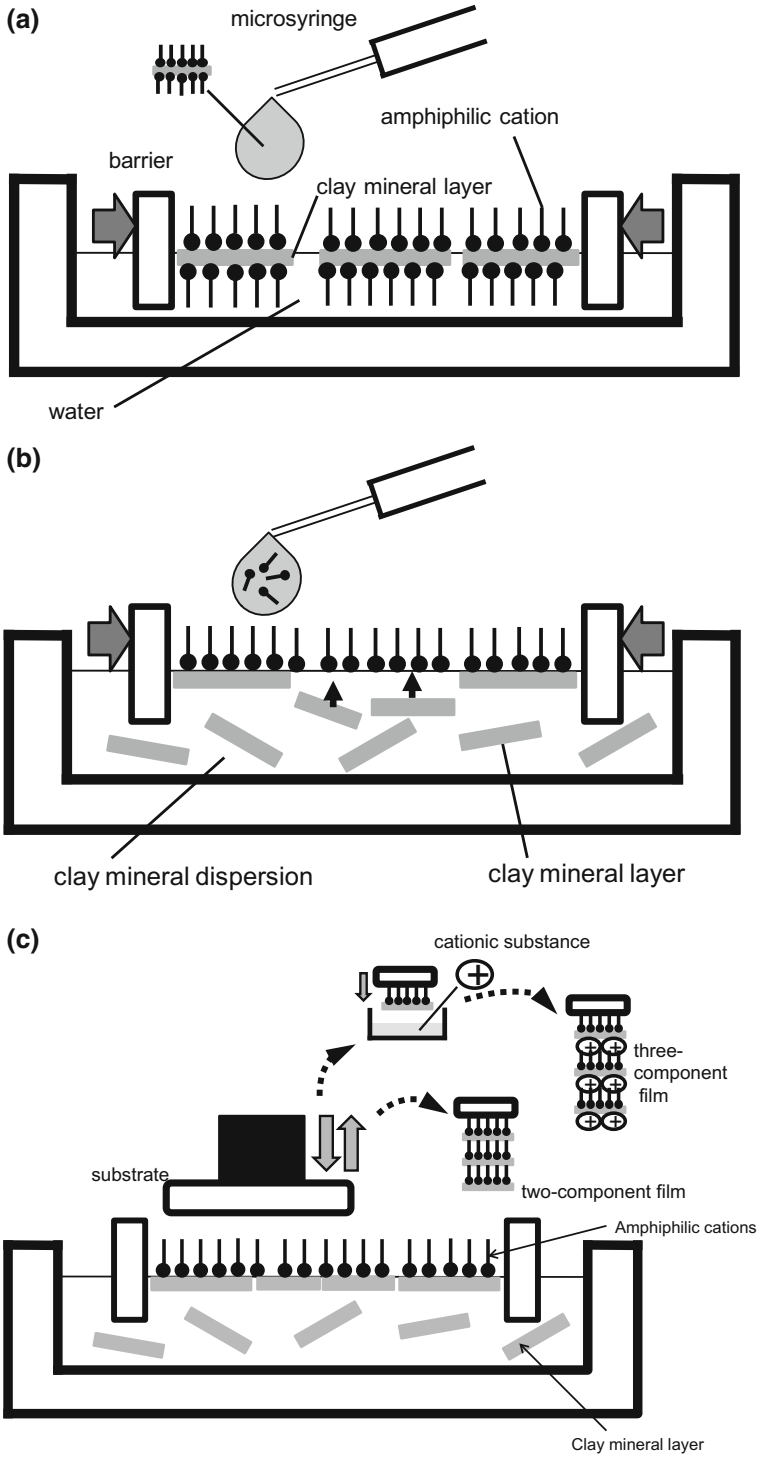
(a)
microsyringe
amphiphilic cation
barrier
clay mineral layer
water
(b)
clay mineral dispersion
clay mineral layer
(c)
cationic substance
three-
component
film
substrate
two-component film
Amphiphilic cations
Clay mineral layer

◀**Fig. 2.7** LB or LS technique for clay film preparation: **a** formation of a floating film of hydrophobic clay mineral particles at the air–water interface, **b** formation of a floating film of amphiphilic cations and clay mineral layers at the air–clay dispersion interface, and **c** deposition of a floating clay film (horizontal lifting) and multilayer fabrication

mineral concentration in the dispersion. If the clay mineral concentration is high, their adsorption rate at the air–water interface is high. Consequently, the individual clay mineral layers are adsorbed on the film of floating amphiphilic cations before evaporation of the solvent and aggregation of the amphiphilic cations. This brings about a low density of amphiphilic cations on the clay mineral layers in the film. Third, even if the amphiphilic cations are water soluble to some extent, a floating hybrid monolayer of clay mineral layers and amphiphilic cations is formed [13]. Fourth, another cationic substance can be deposited on the LB and LS film surfaces as a third component by dipping the surfaces of the films in a solution of the third component after every deposition of the floating hybrid monolayer from the air–water interface, as illustrated in Fig. 2.7c [10–12]. This is because the hybrid LB and LS films possess a cation exchange ability. In the hybrid films, the negative charge of the clay mineral layers is larger than the positive charge of the amphiphilic cations. The density of the third component is dependent on the clay mineral concentration in the dispersion. The three-component films have layered structures, as well as the two-component (clay mineral layers and amphiphilic cations) films.

Recently, formation of clay LB films with amphiphilic anions was reported [14]. A stearic acid solution was spread on the surface of the clay mineral dispersion including divalent cations such as Mg^{2+}. The films cannot be formed with monovalent cations. This suggest that an adduct of clay mineral layers—Mg^{2+} is formed with excess positive charge, which is adsorbed on the floating monolayer of amphiphilic anions.

2.4 Organization of Molecules in the Interlayer Space

Preparation of films is the realization of a two-level organization: that of the clay mineral layers and that of the molecules in the interlayer space. An adequate organization leads to functional films and ultimately to incorporation of these films in devices. Organization of molecules in the interlayer space is a subject with a long history, going back to the pioneering research of Weiss in the 1960s and Lagaly in the 1970s and 1980s, summarized in the Handbook of Clay Science [15].

2.4.1 Alkylammonium Cations

The exchange of alkylammonium cations leads to well organized two-dimensional arrays of alkyl chains in the interlayer space. Monolayers and bilayers can be

obtained depending on the length of the alkyl chain and the charge density of the clay minerals. Idealized pictures are shown in Fig. 2.2. At low charge density, the alkylammonium cations have enough space to lie flat on the siloxane surface, that is to maximize the interaction between the surface and the alkyl ammonium cations. The alkyl chains are positioned with their long axis parallel to the surface. As the charge density increases, the average surface area per charge e is insufficient for such an organization and the alkyl chains are tilted with respect to the surface or they can form a bilayer. These idealized pictures can be perturbed: (1) by thermal motion of the alkyl chains, inducing disorder in their organization; (2) hindered rotations around C–C bonds; (3) the presence of C=C bonds, which prohibit rotation.

2.4.2 *Cationic Organic Dyes*

Cationic organic dyes have some hydrophobic character, limited solubility in water and easily form dimers and aggregates:

$$\begin{aligned} &2\text{dye} \rightleftarrows (\text{dye})_2 \\ &(\text{dye})_2 + \text{dye} \rightleftarrows (\text{dye})_3 \\ &\cdots \\ &(\text{dye})_{n-1} + \text{dye} \rightleftarrows (\text{dye})_n \end{aligned}$$

These reactions are characterized by thermodynamic equilibrium constants, such as

$$K_2 = \frac{[(\text{dye})_2]}{[\text{dye}]^2},$$

$$K_n = \frac{[(\text{dye})_n]}{(\text{dye})^n},$$

where K_n is the global aggregation constant: $K_n = K_2 \cdot K_3 \cdots$. The monomers, dimers, and aggregates have typical UV–Vis spectra and can therefore be easily detected and studied, also in dilute aqueous dispersions. Figure 2.8 gives the structure of typical dyes used in exchange reactions with smectites. Table 2.3 gives the characteristic band maxima for monomers (M), dimers (D), H-aggregates (H), and J-aggregates (J). The distinction between H- and J-dimers and aggregates is in the arrangements of the monomers with respect to each other as shown in Fig. 2.9. Upon interaction of the two monomers, the energy level of the excited state splits into two levels. For the H-dimer, the transition from the ground state to the highest excited state is allowed, causing a blue shift of the absorption band of the H-dimer with respect to that of the monomer. For the J–dimer, the transition to the lowest excited state level is allowed and the absorption band of the J-dimer is red shifted with respect to that of the monomer.

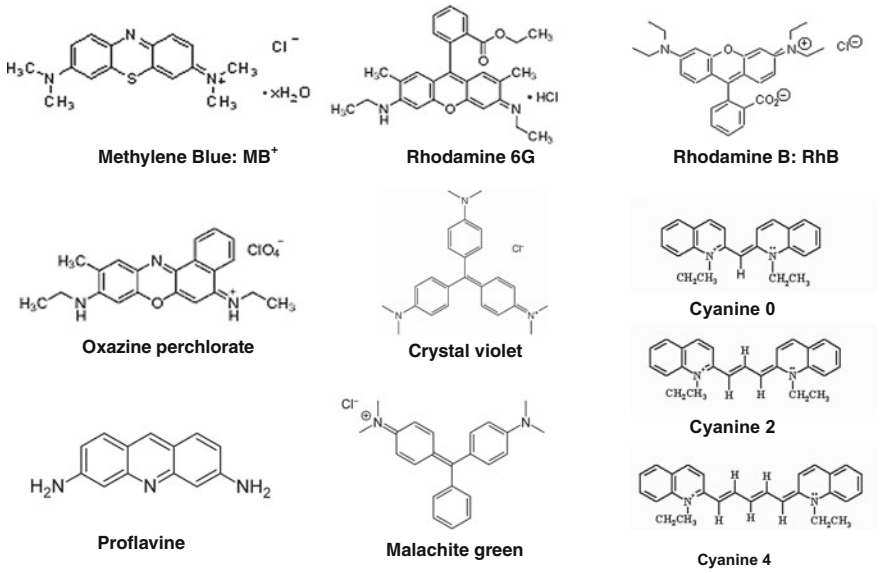

Fig. 2.8 Structure of dye molecules

Table 2.3 Typical band maxima of dyes in dilute aqueous dispersions

Dye[a]	Monomer/nm	Dimer/nm	H-aggregates/nm	J-aggregates/nm
MB	665	605	570	725
Rh6G	528	503		545
Ox4	628	575	475	
CV	590	550		
Cyanin0	520	480		570
Cyanin1	610		500	
Cyanin2	710		560	

[a]*MB* methylene blue; *Rh6G* rhodamine 6G; *CV* crystal violet; *Ox4* oxazine; Cyanin

This aggregation behavior in aqueous solution can be considered as a kind of molecular organization. What happens then in the presence of clay mineral layers in aqueous dispersion and in films?

The organization of cationic organic dyes in the interlayer space of clay mineral films depends mainly on (1) the size and shape of the dye molecules; (2) the layer charge of the clay mineral; and (3) the type of solvent. In dilute aqueous dispersions, the dye molecules are instantaneously adsorbed. The monomer spectrum of the solution is transformed into a spectrum dominated by the band of H-aggregates, as illustrated in Fig. 2.10 for MB. In the next few minutes, a redistribution of the dye molecules over the surface occurs, as seen by the decrease of the 570 nm band of the H-aggregate and the increase of the monomer band and dimer bands. Then the dispersion slowly goes to a metastable equilibrium situation. Cenens et al. [16, 17]

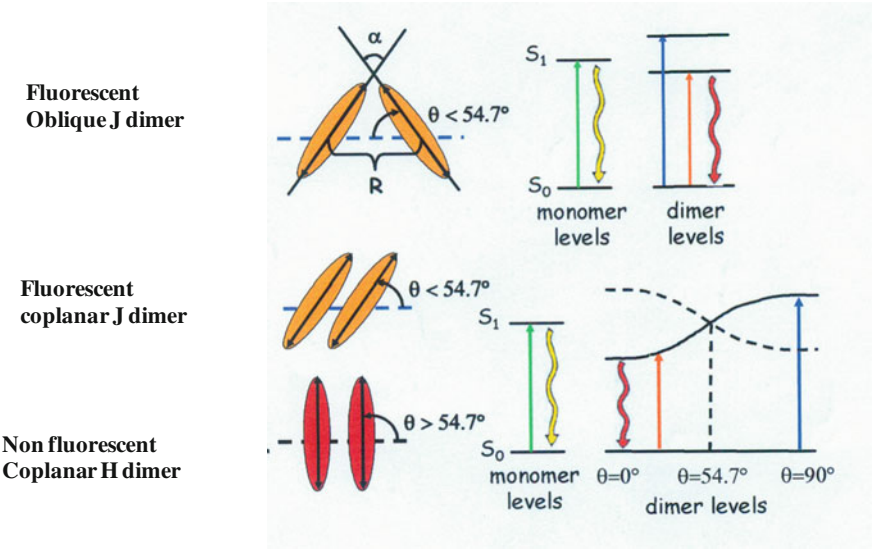

Fig. 2.9 Organization of monomers to obtain H and J dimmers and the corresponding electronic transitions: *vertical arrows up* are allowed absorptions; *curved arrows down* are radiationless transitions

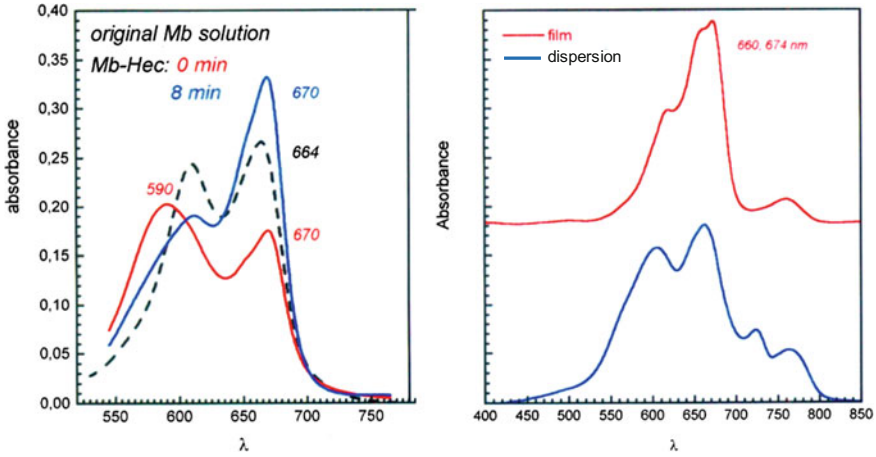

Fig. 2.10 *Left* Spectra of methylene blue (MB) in an aqueous dispersion of hectorite: solution spectrum (*black*), instantaneously after mixing the MB solution with the hectorite dispersion (*red*), and 8 min later (*blue*). *Right* Spectrum of a hectorite-MB dispersion (*blue*) and the corresponding film (*red*). Spectra are taken from [16] and [17]

have tried to calculate the dimerization and trimerization constants of MB and PF in these aqueous dispersions at quasi-equilibrium, assuming that (1) the MB molecules are confined at the surface layer in a layer of 1 nm thickness; and (2) the total surface

area is available for the MB molecules. The data are compared with those in solution in Table 2.4.

The surface areas are assumed to be 775 m^2/g for hectorite and 133 m^2/g for barasym. The latter is a mica-type montmorillonite and only the external surface is available. These data indicate that the dimerization constants at the clay mineral surface are significantly smaller than in aqueous solution. In the latter case dye–dye and dye–water interactions are operating. In the case of dilute aqueous dispersions two forces are added: dye–surface and water–surface interactions. Dye molecules and water molecules compete for interaction with the surface. If water wins, the dye molecules remain surrounded by water molecules and aggregation is favored. If the dye–surface interaction is dominant, dye molecules displace the water molecules at the surface and monomers are favored. The small K_2 (dispersion) values are indicative for the dominance of dye–surface interactions over the water–surface interactions. This competition is moderated by the layer charge density and the position of the layer charge (in the octahedral sheet or in the tetrahedral sheets). Finally, is the total theoretical surface area available for the dye molecules? Cenens et al. [16, 17] have argued on the basis of the decrease of the fluorescence intensity of proflavine with loading that this is only the case for Na^+ and Ca^{2+} exchanged hectorite and Laponite. In the case of K^+ and Cs^+, the available or effective surface area decreased from 775 m^2/g (Na^+-hectorite) to respectively 485 and 580 m^2/g. This means that K^+- and Cs^+-exchanged smectites are only partially swollen in dilute aqueous dispersion.

In films the amount of water is limited. The dye molecules interact predominantly with the clay mineral surfaces. Monomers, dimers, and aggregates have nevertheless been detected. Their relative amounts depend on the loading and the charge density of the clay mineral. At low loadings, the dye molecules maximize

Table 2.4 Dimerization and trimerization constants of MB and PF in water and in dilute aqueous dispersions

Dye	Clay mineral	K_2 (water)	K_2 (dispersion)	K_3 (dispersion)
MB	Hectorite	2000–5900	126–153	
	Barasym[a]			772
PF	Hectorite	395–2700	266–294	

[a]Barasym is a synthetic mica-type montmorillonite; *PF* proflavine

Table 2.5 Estimated sizes of typical dyes

Dye	Width/nm	Height/nm	Length/nm	Width × length/nm^2	Height × length/nm^2
MB	0.47	0.79	1.64	0.87	1.30
CV	0.61	1.50	1.65	1.01	2.48
Cyanin0	0.53	0.97	1.69	0.90	1.64
Cyanin1	0.51	0.96	1.93	0.98	1.85
Cyanin2	0.51	0.95	2.23	1.14	2.19

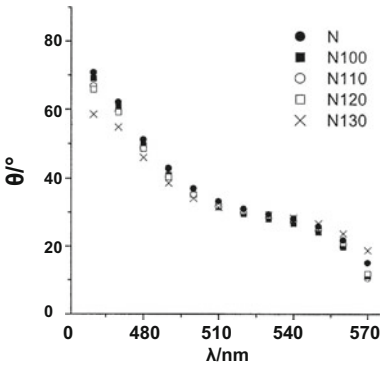

Fig. 2.11 Relationship between the orientation angle θ and the wavelength of absorbed light, calculated for rhodamine6G in reduced charge montmorillonites (from [20] with permission of the Royal Society of Chemistry)

their interaction with the surface with their main molecular axis parallel to the surface. As the loading increases dye molecules form dimers and aggregates with their molecular axes inclined or perpendicular to the surface. Table 2.5 summarizes estimated sizes and occupied surface areas of some typical dyes. They range from 0.87 to 2.48 nm^2 depending on the molecular structure and on how the molecules are situated on the surface. These numbers have to be compared with the average surface area per charge e of the clay minerals: 1e/0.48 nm^2 for mica and 0.82–2.16 nm^2 for smectites with a CEC of 1.5–0.5 mmol/g. It is clear that for a fully exchanged clay mineral, the dye molecules cannot lie flat on the surface. They have to be tilted and they are so close together that intermolecular interaction lead to dimers and aggregates.

This is exactly what is observed. The tilt angles of crystal violet and malachite green were determined to be 55°–59° and 57°–61° respectively on a mica surface [18]. Iwasaki et al. [19] found that the monomers of CV, MB and cyanine dyes were with their main molecular plane parallel with the surface at low loadings, while at higher loadings the J- and H-aggregates were oriented vertically. Bujdak et al. [20] established a relation between the tilt angle and the absorption band maximum of Rh6G in montmorillonite and charge reduced montmorillonite films. This relation is shown in Fig. 2.11. At low loadings the band maximum is at high wavelengths, characteristic of the monomers. The corresponding tilt angle is around 30°. As the loading increases, the band maximum shifts to shorter wavelengths indicative of the presence of H-dimers and H-aggregates. The tilt angles increases to 60°–70°, indicative of an almost perpendicular orientation of the main plane of the molecule with respect to the siloxane surface.

In order to produce functional films, the functionalities of the molecules in the interlayer space (e.g., dipole moment, magnetic moment/susceptibility) must be organized in such a way that an overall functionality (e.g., dipole moment, magnetic dipole moment/susceptibility) is produced in the films. This will not only depend on the organization of the molecules in the interlayer space, but also on the organization of the clay mineral layers, as illustrated in Fig. 2.3. For instance, if one wants to maximize the fluorescence intensity of the films, aggregations of the dye

molecules must be avoided. Dye molecules easily aggregate in water. It might then be advantageous to change to less polar organic solvents such as methanol or ethanol, which are known to suppress aggregation.

2.4.3 Cationic Inorganic Dyes

Inorganic dyes are transition metal ion complexes with intense absorption bands in the visible region of the electromagnetic spectrum. Examples are the bipyridine (bipy) and phenanthroline (phen) complexes. The tris complexes such as $Ru(bipy)_3^{2+}$ and $Ru(phen)_3^{2+}$ are optically active and racemic solutions and enantiomeric solutions can be prepared. Upon exchange in the interlayer space of smectites, the organization of the complexes becomes immediately evident. Exchange with a racemic solution of $Ru(bipy)_3^{2+}$ leads to a monolayer in the interlayer space and the amount adsorbed equals the CEC. In the case of exchange of enantiomeric complexes the amount adsorbed is twice the CEC [21]. For the phenanthroline complexes the opposite occurs: the amount adsorbed from a racemic solution is twice the CEC; that from an enantiomeric solution equals the CEC. This behavior is explained with the hypothesis that the phen complexes in a racemic solution are adsorbed as racemic pairs. Table 2.6 gives a list of complexes which show these effects and complexes which do not [22, 23]. All these complexes are chelates. The chelates with no charge or a positive charge of 1 and 2 (left column of Table 2.6) adsorb as racemic pairs and the amount adsorbed is twice the CEC. A closely packed array of chelates is formed on the surface (Fig. 2.12). When enantiomers of $[Ru(bipy)_3]^{2+}$ are exchanged, empty sites remain on the surface. These sites are used to adsorb selectively the optical antipodes: if Λ-chelates are adsorbed, the clay mineral will selectively adsorb Δ-forms from racemic solutions

Table 2.6 Classification of complexes according to their adsorption behavior on smectites (from Ref. [22] with permission of ACS)

Racemic adsorption (2 × CEC)	Enantiomeric adsorption (2 × CEC)	No stereochemical effect
$[Ni(phen)_3]^{2+}$	$[Ru(bipy)_3]^{2+}$	$[Co(phen)_3]^{3+}$
$[Fe(phen)_3]^{2+}$		$[Co(en)_3]^{2+}$ (en = ethylenediamine)
$[Ru(phen)_3]^{2+}$		*cis*-$[Co(en)_2(Cl_2]^{+}$
$[Fe(phen)_2(CN)_2]$		$[Co(phen)(glyc)_2]^{+}$ (glyc = glycinato)
$[Fe(bipy)_2(CN)_2]$		$[Co(en)(glyc)_2]^{+}$
$[Co(pan)_2]^{2+}$ (pan = pyridylazoresorcinol)		$[Co((en)_2(phegly)]^{2+}$ (phegly = phenylglycinato)
$[Co(pan)_2]^{+}$		$[Co(c\text{-}hexan)_3]^{3+}$ (c-hexan = cyclohexanediamine)

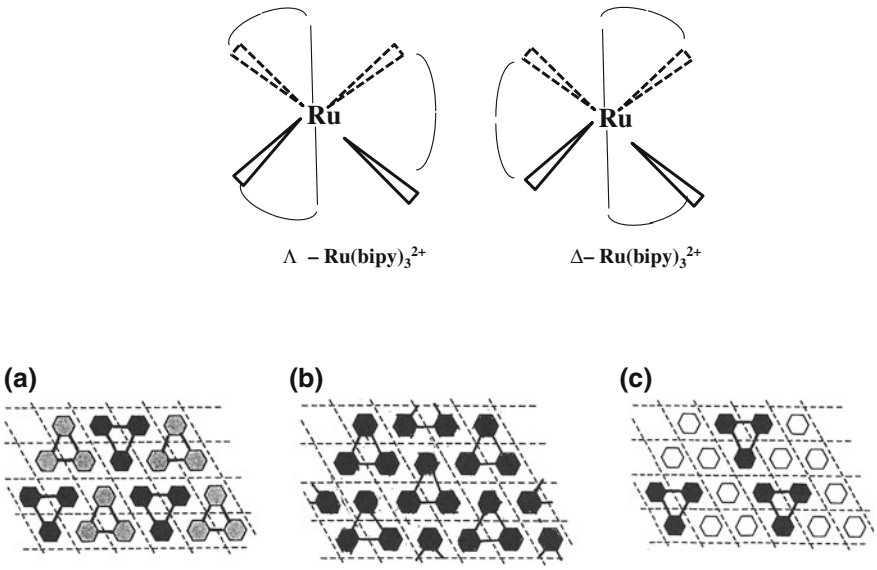

Fig. 2.12 *Upper part* Schematic drawing of lambda (Λ) and delta (Δ) forms of Ru(bipy)$_3^{2+}$. *Lower part* Schematic views of clay layer surfaces occupied with (a) rac – Ru(phen)$_3^{2+}$, (b) Λ- or Δ-Ru(bipy)$_3^{2+}$, and (c) Λ- or Δ-rac – Ru(phen)$_3^{2+}$ (from [23])

and vice versa for adsorbed Δ-chelates. This phenomenon is called chirality recognition [22, 23]. The chelates that do not show this stereochemical behavior have either a too high charge (+3) or the size and the shape of the complexes do not fit the hexagonal hole structure of the siloxane surface on which they are adsorbed.

The importance of this organization is immediately clear when LB films of Ru complexes and smectites are prepared [10]. LB films prepared with saponite and the amphiphilic [Ru(phen)$_2$(dcCl2bpy)] (dcCl2bpy=4,4′-carboxyl-2,2′-bipyridyl didocylester) do not have a second harmonic generation (SHG) signal. However, if the films are made hydrophobic by co-deposition of octadecylammonium cations, an SHG signal is generated, which is more intense with the Λ complex than with the racemic mixture. This is an indirect proof of molecular organization, which is influenced by the surrounding environment in the interlayer space (water, octadecylammonium, surface), a phenomenon that needs a more detailed investigation.

2.5 Organization of Clay Mineral Layers

The organization of particles in films is strongly size- and shape-dependent. A two-dimensional opal structure consisting of hexagonally close-packed, uniform silica spheres is obtained with the LB technique. Multilayers can also be constructed, which act as structures with photonic band gaps [24, 25]. In LB films, the

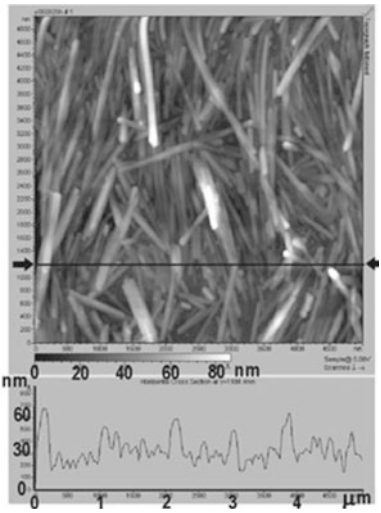

Fig. 2.13 AFM image of a Langmuir–Blodgett film of sepiolite fibers (from [26])

fibers of sepiolite are aligned perpendicularly to the direction of compression, although they overlap to some extent as shown in Fig. 2.13 [26].

For smectites the situation is more complicated for three reasons: (1) a broad range of sizes and shapes is present in the samples; (2) the swelling to complete delamination is an ideal that is difficult, if not impossible, to obtain; (3) impurity particles might be present, either attached to the clay mineral layers or separately. Representative AFM images are shown in Fig. 2.1. One observes that all the clay mineral layers are deposited with their ab plane parallel to the surface of the substrate. This is confirmed with polarized ATR-FTIR spectroscopy of the Si–O and O–H stretching vibrations [27]. The in-plane and out-of-plane Si–O stretching vibrations are at 996 and 1063 cm^{-1}, respectively. The former has a polarization-independent intensity; the out-of-plane vibration is polarization dependent. The structural O–H groups are vibrating almost perpendicularly to the plane of the layers in trioctahedral smectites and parallel with the plane of the layers in dioctahedral smectites.

In all pictures in Fig. 2.1, one sees dark spot and white spots. They are due to the empty spaces between the clay mineral layers and particles or aggregates of clay mineral layers. One observes the differences in sizes and shapes of the different clay minerals. Saponite consists of plate-like and lath-like layers. The layers are more or less randomly oriented and overlap of clay mineral layers also occurs. They have various sizes and shapes and are randomly oriented with some tendency of alignment of the lath-like layers. This is not the case of hectorite which consists solely of lath-like layers. They are overlapping and randomly oriented. Montmorillonite from Wyoming consists of plate-like layers with strongly corrugated edges. Finally, Laponite forms a more or less closely packed array of spherical particles. A comparison of the AFM pictures of sepiolite and hectorite is instructive. The fibers of sepiolite are aligned, while the lath-like layers of hectorite are randomly oriented. It is intriguing to find out the reasons for this difference in behavior. Is it only due to the shape of the minerals?

In cast films, spin-coated films, and LbL films, there is also ordering of clay mineral layers. The evidence comes from spectroscopic analysis of molecules in the interlayer space. For instance, the low spin square planar $[Co(en)_2]^{2+}$ complex in the interlayer space of cast films is characterized by an axially symmetric EPR spectrum. The molecular plane formed by the 2 en ligands and Co^{2+} is parallel with the surface of the clay mineral [28]. The data confirm that the clay mineral layers are deposited with their main surface parallel to the surface of the substrate. However, due to random orientation in the plane and to overlap the films have a rough surface. The surface roughness can reach 10% of the thickness or more, depending on the synthesis conditions [5].

References

1. Breu J, Seidl W, Stoll A, Lange KG, Probst TU (2001) Charge homogeneity in synthetic fluorohectorite. Chem Mater 13:4213–4220
2. Stöter M, Kunz DA, Schmidt M, Hirsemann D, Kalo H, Putz B, Senker J, Breu J (2013) Nanoplatelets of sodium hectorite showing aspect ratios up to 20000 and superior purity. Langmuir 29:1280–1285
3. Lotsch BV, Ozin GA (2008) ACS Nano 2:2065–2074
4. Lotsch BV, Ozin GA (2008) Adv Mater 20:4079–4084
5. Van Duffel B, Schoonheydt RA, Grim CPM, De Schryver FC (1999) Langmuir 15:7520–7529
6. Kotov NA, Meldrum FC, Fendler JH (1994) Langmuir 10:3797–3804
7. Inukai K, Hotta Y, Tomura S, Takahasi M, Yamagishi A (2000) Langmuir 16:7679–7684
8. Tamura K, Setsuda H, Taniguchi M, Yamagishi A (1999) Langmuir 15:6915–6920
9. Umemura Y, Yamagishi A, Schoonheydt RA, Persoons A, De Schryver FC (2001) Langmuir 17:449–455
10. Umemura Y, Yamagishi A, Schoonheydt R, Persoons A, De Schryver F (2002) J Am Chem Soc 124:992–997
11. Umemura Y (2002) J Phys Chem 106:11168–11171
12. Toma LM, Gengler RYN, Cangussu D, Pardo E, Lloret F, Rudolf P (2011) J Phys Chem Lett 2:2004–2008
13. Umemura Y, Shinohara E (2005) Langmuir 21:4520–4525
14. Hussain SA, Chakraborty S, Bhattacharjee D, Schoonheydt RA (2013) Thin Solid Films 536:261–268
15. Lagaly G, Ogawa M, Dékany I (2006) Clay mineral organic interactions. In: Bergaya F, Theng BKG, Lagaly G (eds) Handbook of Clay Science. Elsevier, Amsterdam, pp 309–377
16. Cenens J, Schoonheydt RA, De Schryver FC (1990) Probing the surface of clays in aqurous suspension by fluorescence spectroscopy of proflavine. In: Coyne LM, McKeever SWS, Blake DF (eds) Spectroscopic characterization of minerals and their surfaces, ACS symposium series 415, Chap. 19, pp 378–395
17. Cenens J, Schoonheydt RA (1990) Quantitative absorption spectroscopy of cationic dyes on clays. In: Farmer VC, Tardy Y (eds) Proceedings of the 9th international clay conference, sciences Géologiques Mémoires, vol 85, pp 15–23
18. Fisher D, Caseri WR, Hanher G (1998) J Colloid Interface Sci 198:337–346
19. Iwasaki M, Kita M, Ito K, Kohno A, Fukunishi K (2000) Clays Clay Miner 48:392–399
20. Bujdak J, Iyi N, Kaneko Y, Czimerova A, Sasai R (2003) Phys Chem Chem Phys 5:4680–4685
21. Villemure G (1990) Clays Clay Miner 38:622–630

22. Yamagishi A (1987) J Coord Chem 16:131–211
23. Yamagishi A (1993) Chirality recognition by a clay surface modified with an optically active metal chelate. In: Tamaru K (ed) Dynamic processes on solid surfaces, Chap. 12. Plenum Press, New York, pp 307–347
24. Van Duffel B, Ras RHA, De Schryver FC, Schoonheydt RA (2001) J Mater Chem 11:3333–3336
25. Szekeres M, Kamalin O, Schoonheydt RA, Wostyn K, Persoons A, Dekany I (2002) J Mater Chem 12:3268–3274
26. Umemura Y, Shinohara E, Schoonheydt RA (2009) Phys Chem Chem Phys 11:9804–9810
27. Ras RHA, Johnston CT, Franses EI, Ramaekers R, Maes G, Foubert P, De Schryver FC, Schoonheydt RA (2003) Langmuir 19:4295–4302
28. Schoonheydt RA, Pelgrims J (1983) J Chem Soc. Faraday Trans II 79:1169–1180

http://www.springer.com/978-4-431-56494-2

Inorganic Nanosheets and Nanosheet-Based Materials
Fundamentals and Applications of Two-Dimensional Systems
Nakato, T.; Kawamata, J.; Takagi, S. (Eds.)
2017, VIII, 542 p. 291 illus., 168 illus. in color.,
Hardcover
ISBN: 978-4-431-56494-2